Kank regulates RhoA-dependent formation of actin stress fibers and cell migration via 14-3-3 in PI3K–Akt signaling

Naoto Kakinuma, Badal Chandra Roy, Yun Zhu, Yong Wang, and Ryoiti Kiyama

Signaling Molecules Research Laboratory, National Institute of Advanced Industrial Science and Technology, Tsukuba, Ibaraki 305-8566, Japan

Phosphoinositide-3 kinase (PI3K)/Akt signaling is activated by growth factors such as insulin and epidermal growth factor (EGF) and regulates several functions such as cell cycling, apoptosis, cell growth, and cell migration. Here, we find that Kank is an Akt substrate located downstream of PI3K and a 14-3-3–binding protein. The interaction between Kank and 14-3-3 is regulated by insulin and EGF and is mediated through phosphorylation of Kank by Akt. In NIH3T3 cells expressing Kank, the amount of actin stress fibers is reduced, and the coexpression of 14-3-3 disrupted this effect. Kank also inhibits insulin-induced cell migration via 14-3-3 binding. Furthermore, Kank inhibits insulin and active Akt-dependent activation of RhoA through binding to 14-3-3. Based on these findings, we hypothesize that Kank negatively regulates the formation of actin stress fibers and cell migration through the inhibition of RhoA activity, which is controlled by binding of Kank to 14-3-3 in PI3K–Akt signaling.

Introduction

Phosphoinositide-3 kinase (PI3K)/Akt signaling regulates several important functions in cells, such as cell cycling, apoptosis, cell growth, and cell migration. PI3K activity is induced by insulin and various growth factors such as EGF, PDGF, and insulin-like growth factor 1 (IGF-1). PI3K phosphorylates phosphatidylinositol 4,5-diphosphate (PIP2) to form phosphatidylinositol 3,4,5-triphosphate (PIP3; Franke et al., 1995; Alessi et al., 1996; Dudek et al., 1997; Okano et al., 2000). An oncogene, *v-PI3K*, encoding a catalytic subunit (PI3Kp100α) of PI3K plays an active role in oncogenic transformation (Chang et al., 1997; Aoki et al., 2000), and a tumor suppressor, PTEN, dephosphorylates PIP3 to form PIP2 (Furnari et al., 1998). PIP3 directly as well as indirectly activates Akt, also known as protein kinase B. Activated Akt directly phosphorylates many cellular proteins such as p122RhoGAP, BAD, $p27^{kip1}$, glycogen synthase kinase 3β (GSK3β), and endothelial nitric oxide synthase (Cross et al., 1995; Datta et al., 1997; Fulton et al., 1999; Shin et al., 2002; Hers et al., 2006). v-Akt, an oncogenic gag-fused Akt, has strong kinase activity and transformation activity in rodent and avian cells (Staal, 1987; Bellacosa et al., 1991). Akt phosphorylates serines or threonines in the motif RXRXX(S/T) (Yaffe et al., 2001). Some Akt substrates bind to 14-3-3 in a phosphorylation-dependent manner. For example, BAD itself enhances apoptosis, but when it is phosphorylated by Akt at a serine residue, 14-3-3 binds to it and releases antiapoptotic Bcl-2 family proteins from it (Hsu et al., 1997). When Akt phosphorylates Thr157 of $p27^{kip1}$, a cyclin-dependent kinase inhibitor, phosphorylated $p27^{kip1}$ binds to 14-3-3, and this protein complex is sequestered in the cytoplasm and promotes cell cycling (Sekimoto et al., 2004). These lines of evidence indicate that some Akt substrates exert their functions through association with 14-3-3.

14-3-3 is a family of proteins with seven isoforms in mammals and is ubiquitously expressed. 14-3-3 forms homo- or heterodimers and interacts with various cellular proteins, acting as an adaptor or a molecular chaperone. 14-3-3 interacts with its target proteins in either a phosphorylation-dependent or -independent manner. 14-3-3 itself has no enzymatic activity, although its binding to the target proteins may lead to enhanced apoptosis, cell cycling, cell growth, vesicular transport, cell spreading, or cell migration (Mhawech, 2005). 14-3-3 is associated with several signaling pathways, including PI3K–Akt signaling. It affects not only the interaction between Akt substrates

Correspondence to R. Kiyama: kiyama.r@aist.go.jp

Abbreviations used in this paper: esiRNA, endoribonuclease-prepared siRNA; GSK3β, glycogen synthase kinase 3β; HEK, human embryonic kidney; IGF-1, insulin-like growth factor 1; IMCD, inner medullary collecting duct; IRS, insulin receptor substrate; MBP, maltose-binding protein; PI3K, phosphoinositide-3 kinase; PIP3, phosphatidylinositol 3,4,5-triphosphate; RBD, RhoA-binding domain; RCC, renal cell carcinoma; ROCK; Rho-associated kinase.

The online version of this paper contains supplemental material.

The Rockefeller University Press $30.00
J. Cell Biol. Vol. 181 No. 3 537–549
www.jcb.org/cgi/doi/10.1083/jcb.200707022

and 14-3-3, but also the PI3K–Akt pathway and its upstream factors. 14-3-3θ binds to a catalytic subunit of PI3K (PI3Kp110) and inhibits its activity (Bonnefoy-Bérard et al., 1995). 14-3-3 binds to some proteins upstream of PI3K–Akt, such as insulin receptor substrate (IRS)-1, IGF-1 receptor, EGFR, and integrin β1, and regulates these signals (Craparo et al., 1997; Han et al., 2001; Oksvold et al., 2004). Accordingly, 14-3-3 is important for the regulation of these signaling pathways.

Cell migration plays a central role in many biological and pathological processes such as embryogenesis, tissue repair, cell invasion, and metastasis. PI3K–Akt signaling is also associated with cell migration. PI3K enhances actin remodeling and generates membrane protrusions through activating Rac1 (Scita et al., 2000). PI3K–Akt signals also induce the activation of p70S6K, causing the remodeling of actin and leading to cell migration and cell invasion (Qian et al., 2004). An Akt-interacting protein, Girdin/Akt-phosphorylation enhancer (APE), promotes actin organization and cell motility regulated by Akt (Enomoto et al., 2005). Because of these findings, PI3K signals are considered to be important in cell migration by controlling actin dynamics.

The *Kank* gene, which encodes a kidney ankyrin repeat–containing protein, was originally identified in the region showing a loss of heterozygosity in renal cell carcinoma (RCC); reduced or loss of expression of the gene was observed in RCC tissues and cell lines, and overexpression of Kank resulted in disorganization of β-actin distribution in G-402 cells (Sarkar et al., 2002). In familial cerebral palsy, the region containing the *Kank* gene is often deleted, and this lesion is likely to be associated with this disease (Lerer et al., 2005). An orthologue of Kank in *Caenorhabditis elegans*, VAB-19, is localized at the epidermal attachment structure, and a mutant of this gene causes a phenotype of aberrant actin organization (Ding et al., 2003). Furthermore, Kank inhibits the polymerization of actin and the formation of membrane ruffles induced by active Rac1/cdc42 by directly binding to IRSp53 (unpublished data). From these lines of evidence, Kank is likely to be important for actin dynamics. Kank has a coiled-coil domain at the N terminus and an ankyrin repeat domain at the C terminus. These domains may be involved in protein–protein interactions, and, as it has no apparent enzymatic domain, Kank may work as an adaptor protein. Therefore, identification of Kank-binding proteins is important to find its functions.

Here, we find that Kank is a substrate of Akt and binds to 14-3-3 in a phosphoserine-dependent manner. The interaction between 14-3-3 and Kank is regulated by PI3K–Akt signaling. Furthermore, Kank regulates actin stress fibers and the migration of cells through the inhibition of RhoA, which is controlled by binding of Kank to 14-3-3.

Results

Kank binds to 14-3-3 isoforms γ, ε, η, and θ

To characterize the functions of Kank exerted through its binding proteins, we performed a pull-down assay using an anti–FLAG-tag mAb conjugated to agarose gel with the lysate of human embryonic kidney (HEK) 293T cells transfected with FLAG-Kank expression vector. Then, after the coprecipitated proteins were separated by SDS-PAGE, the bound proteins were subjected to matrix-assisted laser desorption ionization on a time-of-flight mass spectrometry (unpublished data). We found several proteins that bind to Kank, including 14-3-3ε and θ. We first confirmed the interaction between Kank and 14-3-3 by immunoprecipitation and immunostaining (Fig. 1). Endogenous 14-3-3θ was coimmunoprecipitated with an anti-Kank antibody (Fig. 1 A, lane 2), and Kank and 14-3-3 were colocalized in VMRC-RCW cells (Fig. 1 B, panels 1–3).

We then examined which isoform of 14-3-3 bound to Kank (Fig. 1 C). FLAG-tagged Kank and HA-tagged isoforms of 14-3-3, which were expressed in HEK293T cells, were immunoprecipitated with an anti-FLAG antibody. The results indicate that 14-3-3θ strongly bound to Kank, whereas 14-3-3γ, 14-3-3ε, and 14-3-3η also bound to Kank.

Kank binds to 14-3-3 when its 14-3-3–binding motifs are phosphorylated by Akt

14-3-3 interacts with its target proteins in both phosphoserine/phosphothreonine-dependent and -independent manners. Kank contains several candidate 14-3-3-binding motifs with potential phosphorylation at their serine residues. Because a construct of Kank with a deletion of the coiled-coil domain could not bind to 14-3-3 (unpublished data), we focused on two candidate motifs in the coiled-coil domain (149–156 and 162–169: Fig. 2 A). We replaced serine with alanine in the candidate motifs (S154A and S167A) and examined the interaction between the wild type or the mutants ($Kank^{S154A}$ and $Kank^{S167A}$) of Kank and 14-3-3θ (Fig. 2 B). $Kank^{S154A}$ still bound to 14-3-3θ (Fig. 2 B, lane 4), whereas $Kank^{S167A}$ (lane 5) and a mutant containing both mutations ($Kank^{S154A+S167A}$; lane 6) could not bind to 14-3-3θ. Other isoforms of 14-3-3 could not bind to $Kank^{S167A}$ either (unpublished data). To test whether the interaction between Kank and 14-3-3 was direct or indirect, we performed in vitro pull-down assays (Fig. 2 C). All GST-fused 14-3-3 isoforms bound to the wild-type coiled-coil domain (Coil) but not to $Coil^{S167A}$.

The 14-3-3–binding motif at 164–169 has an Akt-phosphorylation motif, and the amino acid Ser167 is a candidate site of phosphorylation by Akt (Fig. 2 A). To determine whether this amino acid was phoshorylated by Akt or not, we performed in vitro phosphorylation assays (Fig. 2 D). First, GST-GSK3β was phosphorylated by Akt, confirming that this Akt kinase activity was sufficient. Under this condition, GST-14b, which contains a 14-3-3–binding motif in Kank, was phosphorylated (Fig. 2 D, lane 3), but GST-14bM (Fig. 2 D, lane 4), which contains the motif with a mutation of S167A, was not phosphorylated. Therefore, the motif at 164–169 was responsible for binding of Kank to 14-3-3, and Ser167 was the site of phosphorylation by Akt.

Because Ser167 was a key amino acid for binding of 14-3-3 and this serine was phosphorylated by Akt in vitro, there was a possibility that the binding between Kank and 14-3-3 was phosphoserine dependent. To examine this, we performed in vitro pull-down assays using maltose-binding

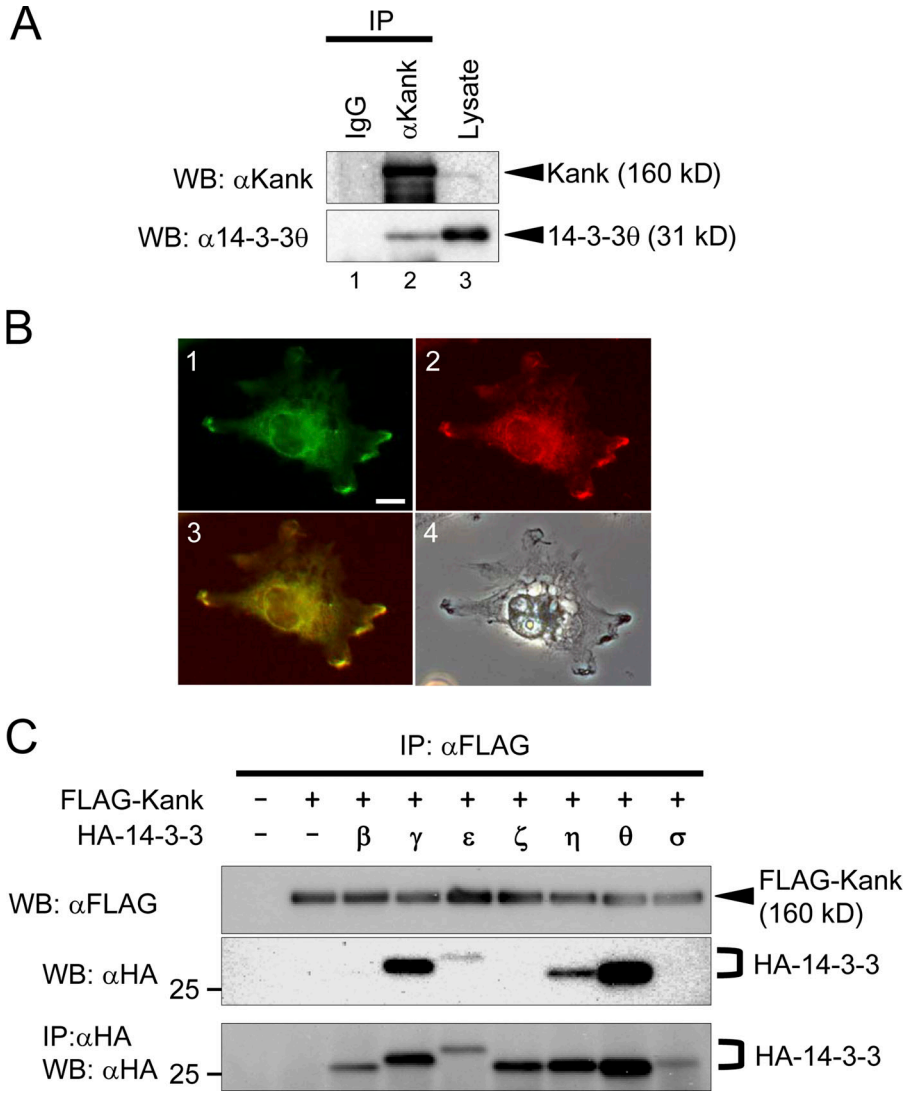

Figure 1. **Kank interacts with 14-3-3 isoforms γ, ε, η, and θ.** (A) Kank interacts with 14-3-3θ. VMRC-RCW cells were lysed and the lysate was immunoprecipitated (IP) with control rabbit IgG (lane 1) or anti-Kank pAb (lane 2). The immunoprecipitates and the lysate (lane 3) were subjected to Western blotting (WB) using the antibodies indicated. (B) Endogenous Kank and 14-3-3 proteins are colocalized in VMRC-RCW cells. A fluorescence image of Kank (green, lane 1), a fluorescence image of 14-3-3 (red, lane 2), a merged image of lanes 1 and 2 (yellow, lane 3), and a light microscope image (lane 4) are shown. Bar, 10 μm. (C) Kank associates with 14-3-3 isoforms γ, ε, η, and θ. HEK293T cells were transfected with the indicated expression vectors. Immunoprecipitation was performed using an anti-FLAG antibody and the bound proteins were detected by Western blotting using the antibodies indicated.

protein (MBP)-fused, phosphorylated, or unphosphorylated coiled-coil domains (Fig. 2 E). Phosphorylation of this protein enhanced the binding to 14-3-3. In addition, the positions of the bands for both Kank and Kank^{S167A} in polyacrylamide gels were shifted after the treatment with calyculin A, a protein phosphatase 2A inhibitor (unpublished data). Therefore, Kank may be phosphorylated at several sites, including Ser167, and its functions could be regulated by phosphorylation of these sites.

Association between Kank and 14-3-3 occurs downstream of PI3K–Akt signaling and is enhanced by growth factors

PI3K–Akt signaling is activated by growth factors such as insulin and EGF. Because Kank was phosphorylated by Akt in vitro (Fig. 2 D, lane 3), the association of Kank and 14-3-3 may be regulated by the PI3K–Akt signals initiated by these growth factors. To examine this possibility, we performed immunoprecipitation assays using PI3K inhibitors (Fig. 3 A). When the assays included the PI3K inhibitors LY294002 (Fig. 3 A, lane 3) and wortmannin (Fig. 3 A, lane 4), both of which reduced the activity of Akt, the association of Kank and 14-3-3θ was significantly reduced. In contrast, when rapamycin, an inhibitor of mammalian target of rapamycin (mTOR), was used (Fig. 3 A, lane 5), the association of these proteins was not affected. Moreover, when the cells were stimulated with insulin or EGF, the association of these proteins was significantly increased (Fig. 3 B, lanes 3 and 5, respectively). Meanwhile, when the cells pretreated with LY294002 were stimulated with the growth factors, the enhancement of the association of Kank and 14-3-3θ was not observed (Fig. 3 B, lanes 4 and 6). These findings indicate that the interaction of Kank and 14-3-3 may occur downstream of these growth factors and be controlled by PI3K–Akt signaling.

Kank inhibits actin stress fibers through 14-3-3

Overexpression of Kank disorganized β-actin distribution in G-402 cells (Sarkar et al., 2002). Because 14-3-3 also affects actin dynamics (Roth et al., 1999; Jin et al., 2004), we examined whether the association between Kank and 14-3-3 affected actin

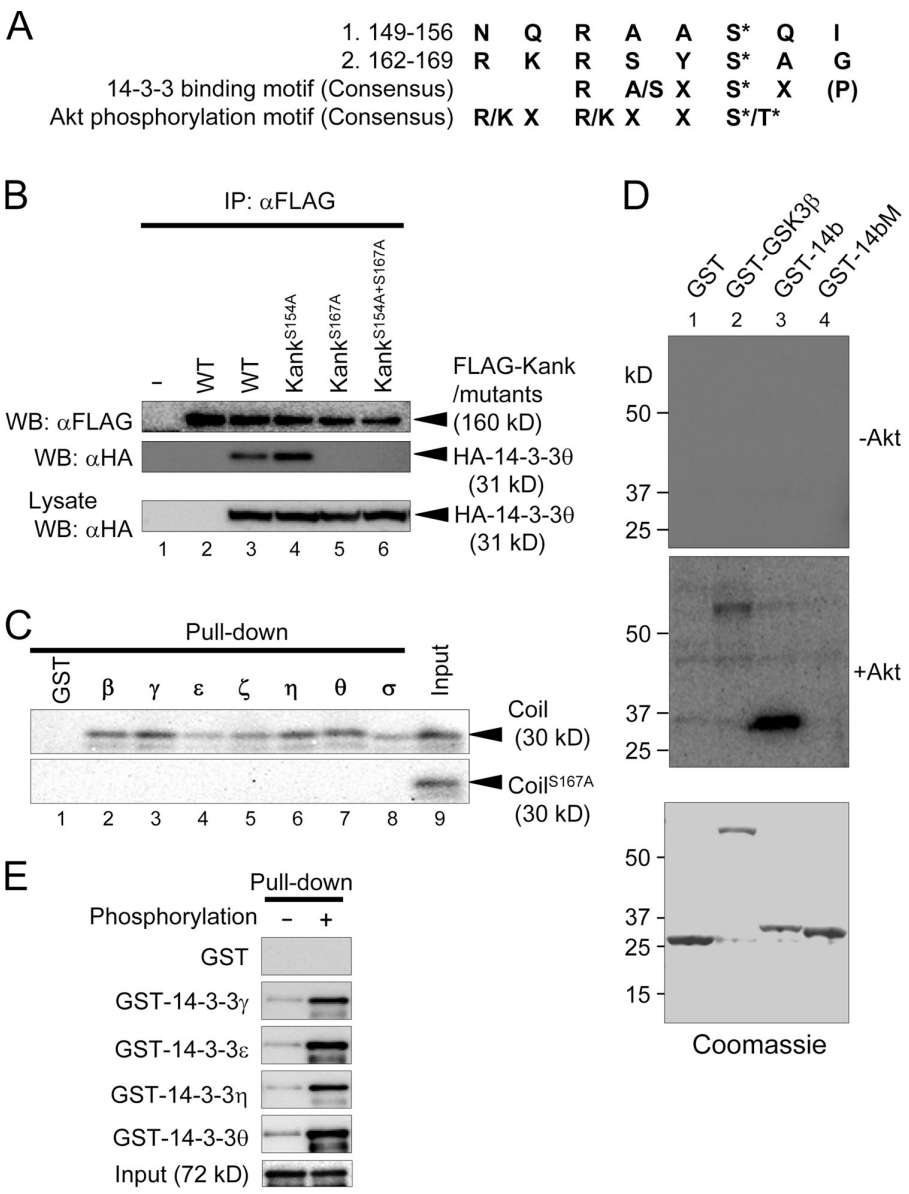

Figure 2. **The 14-3-3–binding motif of Kank is phosphorylated by Akt in vitro and their interaction is phosphorylation dependent.** (A) The amino acid sequences of candidate 14-3-3–binding (149–156 and 162–169) and Akt-phosphorylation (162–167) motifs. The consensus sequences of the 14-3-3–binding motif and the Akt-phosphorylation motif are also shown. (B) Binding of 14-3-3 to wild-type or mutant Kank. Either Ser154 or Ser167, or both, in Kank were replaced by Ala. HEK293T cells expressing wild-type Kank (WT, lanes 2 and 3) or Kank containing mutations (S154A, S167A, and S154A + S167A; lanes 4, 5, and 6, respectively) were subjected to immunoprecipitation followed by Western blotting using the indicated antibodies. (C) The interaction between Kank and 14-3-3 is direct and requires Ser167. GST-fused 14-3-3 isoforms expressed in bacteria were pulled down using the in vitro translated coiled-coil domain (Coil; amino acids 90–360) of Kank or its mutant containing S167A (Coil^{S167A}). Coprecipitates were subjected to Western blotting and detected by staining with streptavidin-HRP. (D) Ser167 of Kank is phosphorylated by Akt in vitro. GST-14b (amino acids 161–171 of Kank, lane 3) and GST-14bM (amino acids 161–171 of Kank containing a mutation of S167A, lane 4), GST, a negative control (lane 1), and GST-GSK3β, a positive control (lane 2), which were all expressed in bacteria, were subjected to phosphorylation by Akt. The samples before (−Akt) or after (+Akt) treatment with Akt along with Coomassie staining are shown. (E) Phosphorylation of the 14-3-3–binding motif by Akt enhances the association of Kank with 14-3-3. MBP-Coil with (+) or without (−) phosphorylation was subjected to pull-down assays with GST 14-3-3 isoforms γ, ε, η, or θ or control GST and the bound MBP-tagged protein was detected using an anti-MBP antibody.

dynamics. Immunofluorescence staining was performed using the cells overexpressing Kank or Kank mutants in the presence or absence of 14-3-3θ (Fig. 4). When Kank was overexpressed, the number of cells with clear actin stress fibers was significantly decreased. Kank$^{\Delta coil}$, a mutant with a deletion in the coiled-coil domain, had little effect on actin stress fibers (Fig. 4 A; quantified in Figs. 4 B and S1 A, available at http://www.jcb.org/cgi/content/full/jcb.200707022/DC1). Expression of Kank^{S167A}, which lacked the ability to bind to 14-3-3, slightly decreased the number of cells with higher levels of actin stress fibers (Fig. 4 B, lane 4), but the number was higher than that with Kank expression (Fig. 4 B, lane 2). The inhibitory effect of Kank on the formation of actin stress fibers was eliminated by the coexpression of 14-3-3θ (Fig. 4 B, lane 6). Furthermore, knockdown of Kank enhanced F-actin in NIH3T3 cells (Fig. S1 B). Based on these findings, we hypothesized that Kank inhibits the formation of actin stress fibers and that one of the potential mechanisms is the interaction between Kank and 14-3-3θ.

Kank inhibits insulin-stimulated cell migration through 14-3-3

Cell migration plays a central role in many biological and pathological processes such as embryogenesis, tissue repair, tumor invasion, and metastasis. When cells are moving, the lamellipodial and filopodial membrane protrusions are formed at the leading edge after the activation of Rac1 or cdc42. PI3K and PTEN are polarized in migrating cells and PI3K is accumulated at the leading edge of the cells (Ridley et al., 2003). Girdin/APE and p70S6K, downstream effectors in PI3K–Akt signaling, regulate cell migration (Qian et al., 2004; Enomoto et al., 2005). Rather, 14-3-3 enhances cell migration (Rodriguez and Guan, 2005). Because the function of Kank through 14-3-3 is likely to be exerted downstream of PI3K–Akt and may affect actin organization, Kank may inhibit cell migration. To examine this, we performed cell migration assays (Figs. 5 and S2 B, available at http://www.jcb.org/cgi/content/full/jcb.200707022/DC1). We generated HEK293 cells expressing FLAG-Kank or

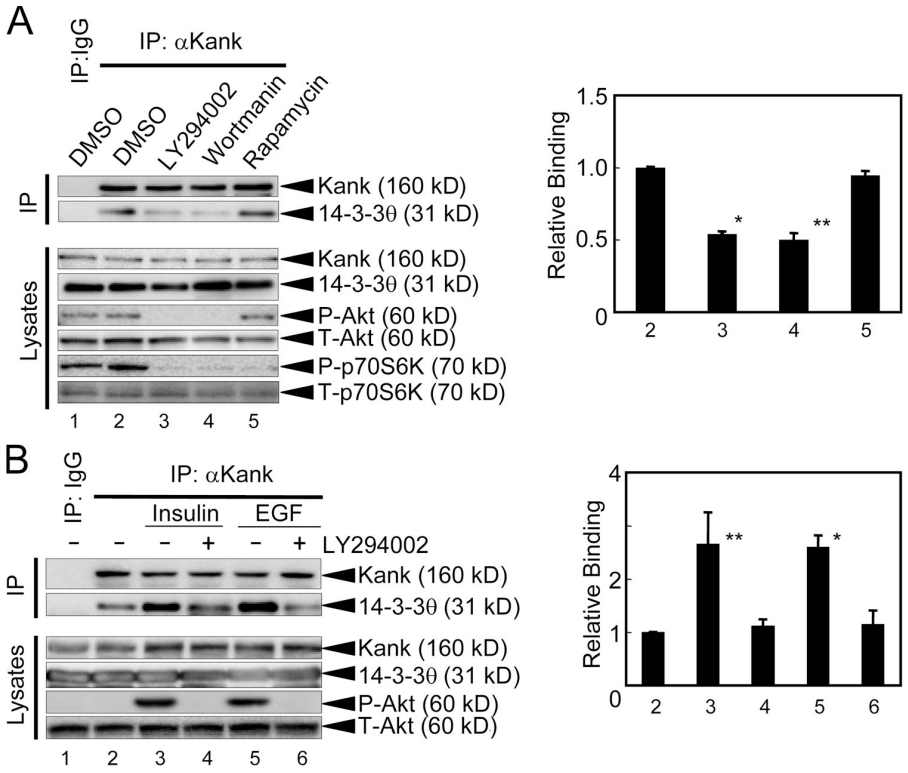

Figure 3. **The interaction between 14-3-3 and Kank occurs downstream of PI3K–Akt signaling and is enhanced by growth factors.** (A) The association between 14-3-3 and Kank occurs downstream of the PI3K–Akt signaling. After IMCD cells were treated with vehicle (DMSO, lanes 1 and 2), 50 µM LY294002 (lane 3), 100 nM wortmannin (lane 4), or 0.2 nM rapamycin (lane 5) for 24 h, the cells were collected, lysed, and subjected to immunoprecipitation using anti–mouse Kank antibody. The results of Western blotting are shown on the left and the intensities of the bands quantified using an ImageQuant image analyzer are shown on the right. *, $P < 0.01$ compared with the vehicle; **, $P < 0.05$ compared with the vehicle. (B) The interaction between 14-3-3 and Kank is enhanced by insulin and EGF. IMCD cells either pretreated (lanes 4 and 6) or not pretreated (lanes 3 and 5) with 50 µM LY294002 (LY) were treated with 10 µg/ml insulin (lanes 3 and 4) or 10 ng/ml EGF (lanes 5 and 6). The experiments were performed as described in A. *, $P < 0.01$ compared with the control; **, $P < 0.05$ compared with the control. The results shown are the mean ± SD of at least triplicate experiments.

FLAG-Kank^{S167A} using tetracycline-inducible HEK293 cells, TREx-293 cells, in which the expression of these genes can be induced with tetracycline (Fig. 5 C). The expression of Kank inhibited cell migration, although Kank^{S167A} had little effect on cell migration (Fig. 5, A and B). Kank transiently expressed in HEK293 cells also inhibited cell migration, whereas Kank^{S167A} had little effect on cell migration (Fig. S2 B, 2 and 3, white columns). Furthermore, the Kank knockdown cells using endoribonuclease-prepared siRNA (esiRNA) in which little endogenous Kank protein was expressed (Fig. 5 E, lane 2) showed upregulation of cell migration (Fig. 5 D, lane 2). Because Shanley et al. (2004) found that insulin induces cell migration in the corneal epithelium, we examined whether Kank inhibits insulin-dependent cell migration in TREx-293 cells (Fig. 5). Insulin enhanced cell migration about twofold, and insulin-stimulated cell migration was significantly reduced upon the expression of Kank (Fig. 5 A, lane 4). However, Kank^{S167A} did not show any inhibitory effect on insulin-induced cell migration (Fig. 5 B, lane 4). Kank and Kank^{S167A} transiently expressed in HEK293 cells also showed a similar tendency (Fig. S2 B, black columns). Furthermore, knockdown of Kank slightly enhanced insulin-induced cell migration (Fig. 5 D, lane 4). In contrast, coexpression of 14-3-3θ with Kank abolished this effect (Fig. S2 A). These results suggest that Kank inhibits insulin-induced cell migration through 14-3-3.

Kank inhibits insulin-induced RhoA activation through 14-3-3

Actin stress fibers are one of the major cytoskeletal structures, and GTP-loaded RhoA stimulates actin stress fibers in response to growth factors (Ridley and Hall, 1992). An active form of RhoA, RhoA^{G14V}, enhances the formation of actin stress fibers and vinculin-containing focal adhesions (Nobes and Hall, 1995). RhoA also controls cell motility and cell invasion (Takaishi et al., 1993; Yoshioka et al., 1999; Kurokawa and Matsuda, 2005). When cells are moving, RhoA activates migrating cells not only at the tail but also at the leading part. Because Kank inhibits actin stress fibers and cell migration, we examined whether Kank inhibits RhoA activity by pull-down assays using a GST-fused RhoA-binding domain (RBD) of rhotekin (GST-RBD; Fig. 6). When Kank was expressed, the amount of active RhoA was significantly reduced (Fig. 6 A, lane 3). In contrast, when Kank^{S167A}, which is unable to bind to 14-3-3, was expressed, the amount of active RhoA was not markedly affected (Fig. 6 A, lane 4). Furthermore, knockdown of Kank significantly increased the amount of active RhoA (Fig. 6 A, lane 2). When 14-3-3θ was expressed, the amount of active RhoA was slightly increased (Fig. 6 B, lane 2). Moreover, coexpression of 14-3-3θ with Kank abolished the effect of Kank, and the level of active RhoA was decreased (Fig. 6 B, lane 3). We generated stable NIH3T3 cell lines expressing tetracycline-inducible GFP-Kank or GFP-Kank^{S167A} and used them to study the role of Kank in active RhoA (Fig. 6, C and D). When GFP-Kank was expressed, the amount of active RhoA was significantly reduced (Fig. 6, C and D, lanes 1 and 3), whereas the expression of GFP-Kank^{S167A} had little effect on the amount of active RhoA (Fig. 6, C and D, lanes 5 and 7), as was observed with the transient expression of Kank or its mutant (Fig. 6 A).

Insulin activates RhoA in rat adipocytes (Karnam et al., 1997). Here, we also observed that insulin increased the amount of active RhoA (Fig. 6, C and D). The expression of GFP-Kank significantly inhibited the increase of active RhoA stimulated

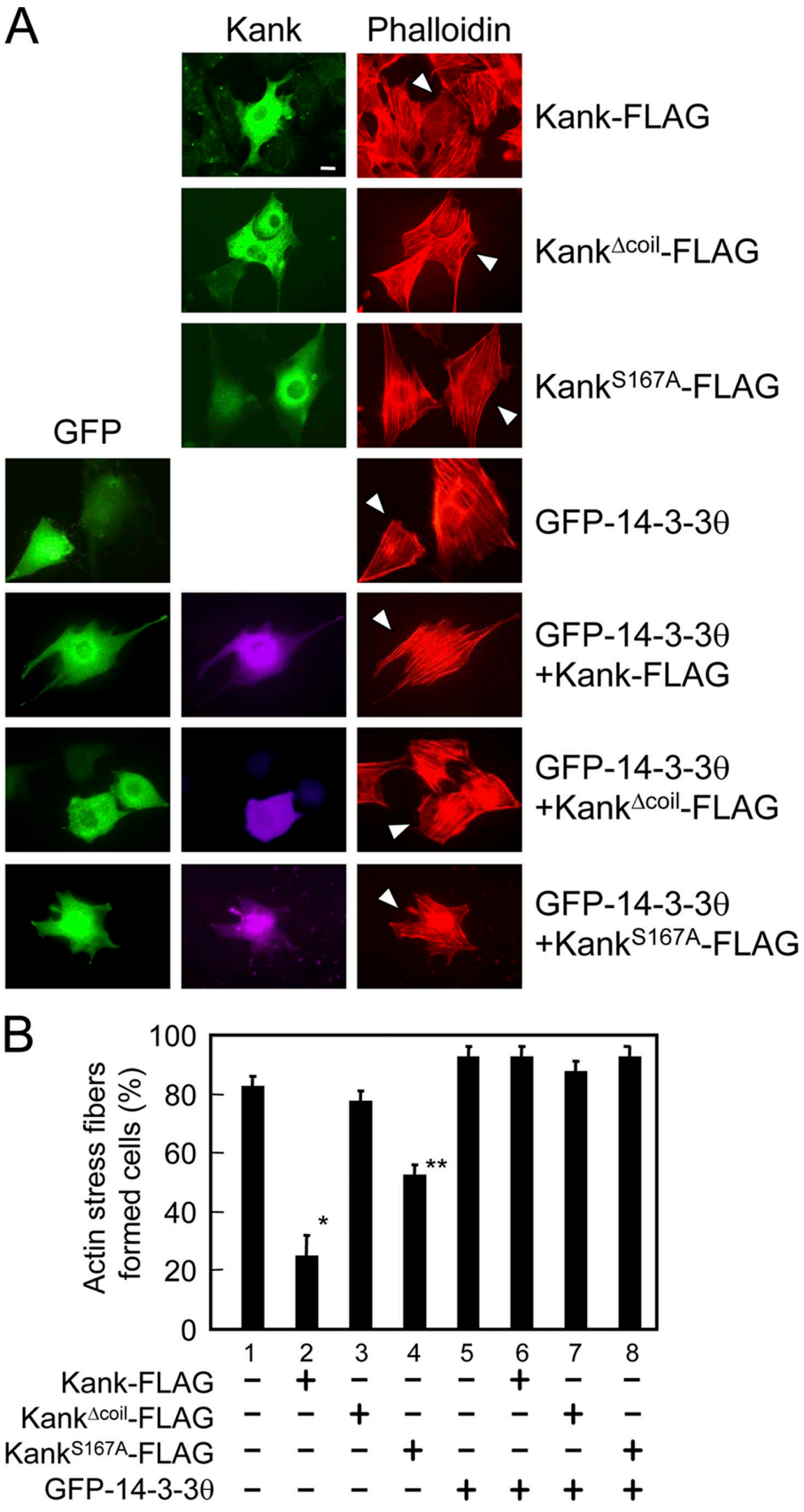

Figure 4. **Kank inhibits the formation of actin stress fibers through 14-3-3.** (A) Kank inhibits the formation of actin stress fibers. Kank or its mutants (Kank$^{\Delta coil}$-FLAG, Kank with deletion of amino acids 90–360, and Kank^{S167A}-FLAG) were expressed with or without 14-3-3θ in NIH3T3 cells. The cells were incubated with an anti-Kank pAb or anti-Kank mAb together with an anti-GFP antibody. Kank protein was detected using Alexa Fluor 488–conjugated goat anti–rabbit IgG (green, top middle) or Cy5-conjugated goat anti–mouse antibody (purple, bottom middle). GFP protein was detected using Alexa Fluor 488–conjugated goat anti–rabbit IgG (green, left). F-actin was stained with TRITC-conjugated phalloidin. Arrowheads indicate the cells expressing the transfected vectors. Bar, 10 µm. (B) The number of the cells with actin stress fibers was quantified. Kank and its mutants were transiently expressed and the cells were stained as described in A. 100 cells expressing the transfected genes were examined and the results shown are the means ± SD of three independent experiments. *, $P < 0.01$ compared with the control; **, $P < 0.05$ compared with the control.

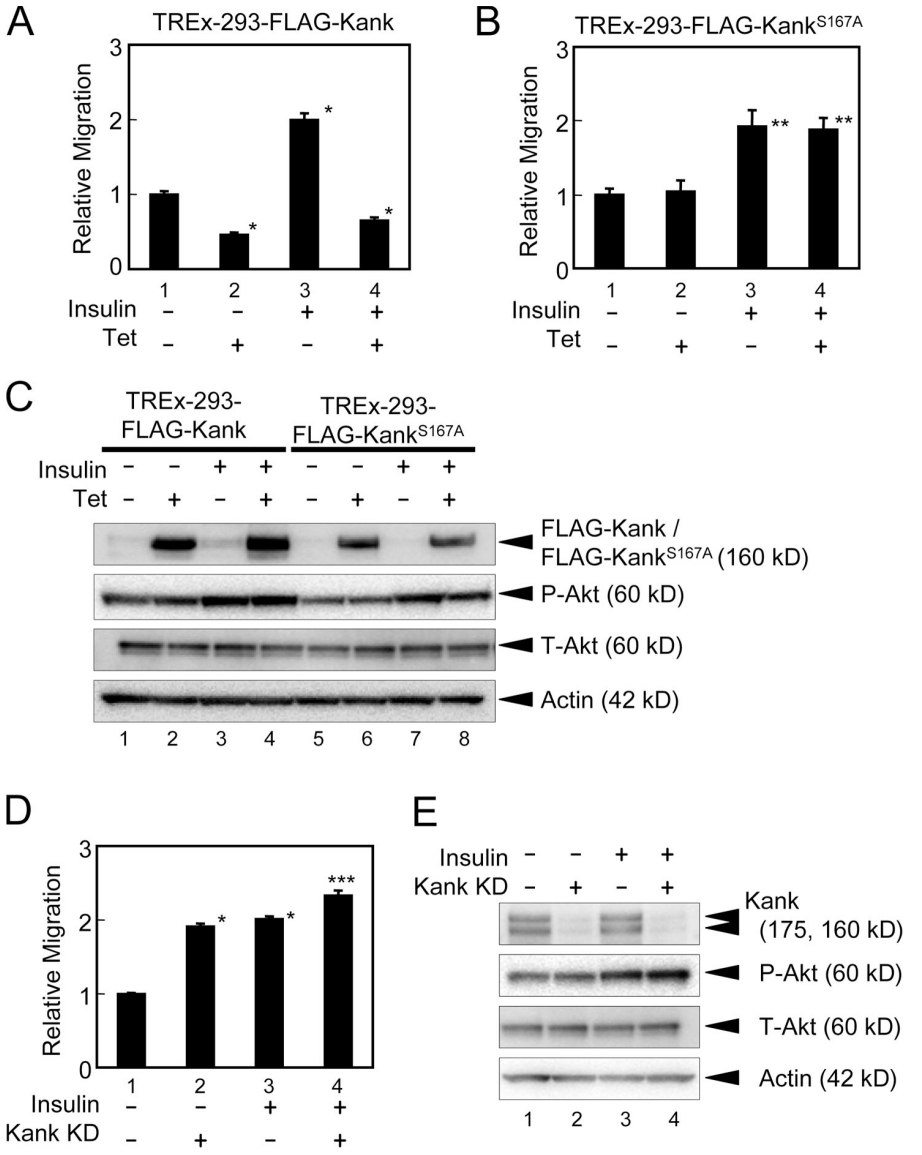

Figure 5. **Kank inhibits cell migration through 14-3-3 and partially inhibits insulin-mediated cell migration.** (A and B) Tetracycline-inducible TREx-293 cells stably expressing Kank (A) or Kank^{S167A} (B) were subjected to cell migration assays using TransWell. TREx-293 cells expressing tetracycline-inducible FLAG-Kank or FLAG-Kank^{S167A} with (lanes 3 and 4) or without (lanes 1 and 2) insulin (10 µg/ml) stimulation were used for cell migration assays. The ratios of migration compared with the control were calculated. The results shown are the means ± SD of triplicate experiments. Tet, tetracycline induction. *, $P < 0.01$ compared with the control ; **, $P < 0.05$ compared with the control. (C) The expression of FLAG-Kank and FLAG-Kank^{S167A} is induced in tetracycline-inducible TREx-293 cells. The expression of FLAG-Kank (lanes 1–4) and FLAG-Kank^{S167A} (lanes 5–8) with or without the treatment with 10 µg/ml insulin and/or tetracycline was examined by Western blotting. (D) Knockdown of Kank enhances cell migration. The esiRNA of Kank (Kank KD, lanes 2 and 4) and control esiRNA (lanes 1 and 3) were prepared as described in Materials and methods and transfected into HEK293 cells. Cell migration assays were performed using these transfected cells in the presence (lanes 3 and 4) or absence (lanes 1 and 2) of 10 µg/ml insulin. The relative migration was calculated as described in A. *, $P < 0.01$ compared with the control; ***, $P < 0.01$ compared with the control and $P < 0.05$ compared with Kank KD. (E) The expression of endogenous Kank is decreased by the esiRNA of Kank. The expression levels of endogenous Kank were determined by Western blotting. The cells were transfected and stimulated as described in D.

by insulin (Fig. 6, C and D, lanes 2 and 4), whereas GFP-Kank^{S167A} had little effect on the level of active RhoA (Fig. 6, C and D, lanes 6 and 8). We established stable NIH3T3 cells in which knockdown of Kank was induced with tetracycline and the amount of Kank was reduced by ~70% (Fig. 6, E and G, lanes 3 and 4). Using this cell line, we performed GST-RBD pull-down assays for the detection of active RhoA. In the cells in which Kank was knocked down, the amount of active RhoA was significantly increased, as shown in Fig. 6 (A, lane 2; and Fig. 6, E and F, lane 3), whereas the level of active RhoA did not show significant differences between the control and knockdown cells when the cells were stimulated with insulin (Fig. 6, E and F, lanes 2 and 4).

Meanwhile, PI3K signals may be related to RhoA activation. Qiang et al. (2004) showed an IGF-1–induced GTP-RhoA increase in myeloma cells, and this induction was inhibited by LY294002 (Qiang et al., 2004). However, Karnam et al. (1997) showed that RhoA was translocated to the membrane through PI3K signaling after insulin stimulation in rat adipocytes, but GTP loading of RhoA was not inhibited by wortmannin (Karnam et al., 1997). Here, we investigated whether or not the amount of active RhoA is increased through PI3K–Akt signaling after stimulation with insulin in NIH3T3 cells (Fig. 6 H). When NIH3T3 cells were pretreated with LY294002, the level of active RhoA was significantly decreased (unpublished data). Furthermore, constitutively active Akt increased the level of active RhoA (Fig. 6, H and I, lane 2). We also assessed active RhoA levels in the cells in which Kank and Kank^{S167A} were coexpressed with constitutively active Akt. The overexpression of Kank significantly inhibited active Akt-dependent RhoA activation, whereas Kank^{S167A} had little effect (Figs. 6, H and I, lanes 3 and 4).

Kank regulates cell migration by inhibition of RhoA activity

C3 transferase is an ADP-ribosyltransferase of *Clostridium botulinum* specific to Rho that affects both actin stress fibers and cell morphology and inhibits cell motility (Paterson et al., 1990;

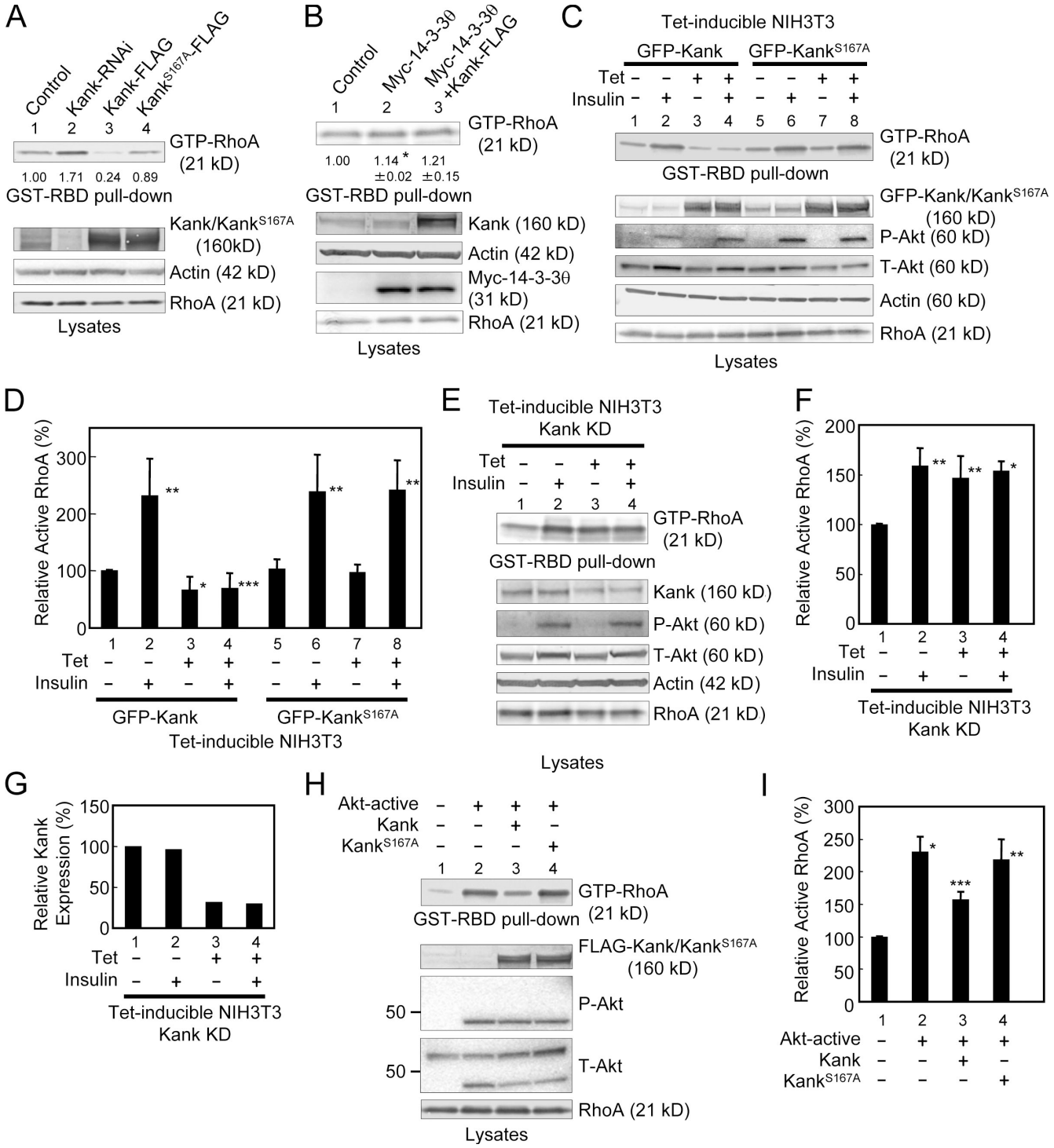

Figure 6. **Kank inhibits PI3K–Akt–dependent activation of RhoA through 14-3-3.** (A) Kank inhibits active RhoA through 14-3-3. RNAi for knockdown of Kank (Kank-RNAi, lane 2), Kank-FLAG (lane 3), or Kank^{S167A}-FLAG (lane 4) was transfected in NIH3T3 cells, and GST-RBD pull-down assays were performed to determine the expression levels of active RhoA (GTP-RhoA). The amounts of active RhoA in Western blot data were quantified, and the amounts relative to that of the control (lane 1) are shown below the GTP-RhoA data. (B) Overexpression of 14-3-3θ blocks Kank function in RhoA activation. After electroporation as indicated in NIH3T3 cells, a GST-RBD pull-down assay was performed to quantify the amount of active RhoA (GTP-RhoA). The amounts of active RhoA in Western blot data were quantified and the amounts relative to that of the control (lane 1) are shown below the GTP-RhoA data. The results shown are the mean ± SD of triplicate experiments. *, $P < 0.01$ compared with the control. (C and D) GFP-Kank but not GFP-Kank^{S167A} inhibits insulin-dependent RhoA activation. We generated tetracycline-inducible stable cells expressing GFP-Kank (lanes 1–4) or GFP-Kank^{S167A} (lanes 5–8) using NIH3T3 cells and tested the levels of active RhoA in these cells with (lanes 2, 4, 6, and 8) or without (lanes 1, 3, 5, and 7) insulin stimulation. Western blotting results are shown in C. The levels of active RhoA, shown in C, were quantified, and the relative levels of active RhoA compared with the control (lane 1) are shown in D. The results shown are the mean ± SD of triplicate experiments. *, $P < 0.01$ compared with the control; **, $P < 0.05$ compared with the control; ***, $P < 0.05$ compared with the control stimulated with insulin. (E and F) Knockdown of Kank significantly enhances the level of active RhoA. We generated a tetracycline-inducible RNAi cell line derived from NIH3T3 cells for knockdown of Kank and performed GST-RBD pull-down assays. Western blotting results are shown in E. The levels of active RhoA, shown in E, were quantified as described in D and are shown in F. *, $P < 0.01$ compared with the control; **, $P < 0.05$

Takaishi et al., 1993). Rho activates Rho-associated kinase (ROCK), and ROCK is inhibited by a specific inhibitor, Y-27632 (Amano et al., 2000). The Rho–ROCK signaling pathway is involved in organization of the actin cytoskeleton and cell migration (Itoh et al., 1999; Amano et al., 2000; Worthylake and Burridge, 2003). Knockdown of *Kank* resulted in enhanced cell migration (Fig. 5 D). If this effect depends on the activation of RhoA, it should be inhibited by C3 transferase and Y-27632. To examine this, we performed cell migration assays using stable HeLa cells expressing human *Kank* RNAi (Fig. 7). When the cells were treated with cell-permeable C3 transferase, which can be transported through the plasma membrane, the level of active RhoA was significantly reduced in both the control and knockdown cells (Fig. 7, A and B, lanes 2 and 4). The migration of cells was slightly reduced in the control cells by the treatment with cell-permeable C3 transferase and Y-27632 (Fig. 7 C, lane 1). In contrast, the migration of cells was markedly reduced in Kank knockdown cells by the treatment with cell-permeable C3 transferase or Y-27632 (Fig. 7 C, respective columns in lane 3). The migration of cells was inhibited for both control and Kank knockdown cells when they were treated with cell-permeable C3 transferase or Y-27632 after stimulation with insulin (Fig. 7 C, respective columns in lanes 2 and 4). The cells transiently expressing *Kank* RNAi (Kank KD) showed a similar tendency in HEK293 cells (Fig. S3, available at http://www.jcb.org/cgi/content/full/jcb.200707022/DC1). These findings suggest that Kank inhibits cell migration through the regulation of RhoA signaling. Moreover, Kank^{S167A} did not affect RhoA activity and cell migration (Figs. 5 B, 6, and S2 B), which suggests that Kank regulates cell migration through RhoA signaling mediated by 14-3-3 binding.

Discussion

PI3K–Akt signaling regulates multiple biological processes such as cell cycling, apoptosis, cell growth, and cell migration. This signaling is activated by insulin and various growth factors, such as EGF, PDGF, and IGF-1, and the phosphorylation of Akt substrates is involved in some of these cellular functions (Franke et al., 1995; Alessi et al., 1996; Dudek et al., 1997; Okano et al., 2000). We show here that Kank was also phosphorylated by Akt in vitro (Fig. 2 D) and that the apparent molecular weights of Kank and Kank^{S167A} were altered by treatment with a protein phosphatase 2A inhibitor, calyculin A (unpublished data). These results indicate that Kank is phosphorylated not only within its 14-3-3 binding motif but also at other serines and/or threonines, and this phosphorylation may be regulated by protein phosphatase 2A and other serine/thereonine kinases. We found that Kank bound to 14-3-3 and that this interaction was enhanced by the phosphorylation of Kank in vitro by Akt (Fig. 2 E). Furthermore, PI3K inhibitors, LY294002 and wortmannin, significantly reduced the level of this interaction, whereas the stimulation of cells with insulin and EGF significantly enhanced it (Fig. 3, A and B). These lines of evidence suggest that PI3K–Akt signaling may control the function of Kank through 14-3-3 by phosphorylation of a site within the 14-3-3–binding motif. Lack of phosphorylation of the 14-3-3–binding motif and endogenous Kank resulting from treatment with LY294002 resulted in weak binding of Kank to 14-3-3 in vitro and in vivo (Fig. 2, C and E; and Fig. 3, A and B). Raf-1 binds to 14-3-3 in a phosphorylation-dependent manner (Muslin et al., 1996). Although recombinant bacterial Raf-1, which is likely to be unphosphorylated, also binds to 14-3-3 (Li et al., 1995), the complex may not be functional. Similarly, the interaction between the unphosphorylated 14-3-3–binding motif in Kank and 14-3-3 may be nonfunctional or may be so weak at this interaction that Kank is not fully functional through 14-3-3. However, Kank bound to all isoforms of 14-3-3 in vitro, whereas Kank bound to the isoforms γ, ε, η, and θ in vivo (Figs. 1 C and 2 C). This difference may be caused by the state of folding of Kank in live cells. In fact, HSP70 is one of the Kank-binding proteins (unpublished data). This protein, as well as 14-3-3, may act as a molecular chaperone and may affect the folding of Kank. The folding of Kank may be one of the important factors for the interaction between Kank and 14-3-3, and the difference of the abilities of the isoforms of 14-3-3 to bind to Kank may result in different functions.

RhoA, a small GTPase, is critical for the formation of actin stress fibers and cell migration (Ridley and Hall, 1992; Takaishi et al., 1993; Nobes and Hall, 1995; Yoshioka et al., 1999; Kurokawa and Matsuda, 2005). Active RhoA, GTP-loaded RhoA, activates downstream effectors ROCK and Dia, resulting in organization of the actin cytoskeleton (Maekawa et al., 1999; Fukata et al., 2001; Wallar and Alberts, 2003). RhoA is activated in the tail and the leading edge of migrating cells (Kurokawa and Matsuda, 2005), and the degree of cell invasion is significantly reduced when the cells are treated with a RhoA inhibitor, C3 transferase (Yoshioka et al., 1999). These facts indicate that RhoA activation is tightly related to cell migration. However, the relationship between 14-3-3 and actin polymerization has not been thoroughly investigated. However, 14-3-3 enhanced actin cytoskeleton formation in *Saccharomyces cerevisiae* (Roth et al., 1999; Lottersberger et al., 2006). 14-3-3 has many binding partners, including those related to actin polymerization (Jin et al., 2004; Pozuelo Rubio et al., 2004). Among them, p190RhoGEF and AKAP-Lbc, which are both activators of RhoA, were identified as 14-3-3–binding partners (Zhai et al., 2001; Diviani et al., 2004). Furthermore, cofilin, an actin depolymerization factor, and SSH1L, a cofilin phosphatase, both

compared with the control. (G) The level of endogenous Kank is decreased by the induction of Kank RNAi in NIH3T3 cells. The levels of endogenous Kank, shown in E, were quantified, and the relative levels of Kank compared with the control (lane 1) were calculated. (H and I) Active Akt increases the level of active RhoA, whereas Kank inhibits this activation. Plasmids expressing active Akt and Kank (lane 3), Kank^{S167A} (lane 4), or active Akt alone (lane 2) were electroporated into NIH3T3 cells as indicated, and GST-RBD pull-down assays were performed to examine the levels of active RhoA. The results of Western blotting are shown in H. The levels of active RhoA, shown in H, were quantified as described in D and shown in I. *, $P < 0.01$ compared with the control; **, $P < 0.05$ compared with the control; ***, $P < 0.01$ compared with the control and $P < 0.05$ compared with the active Akt alone.

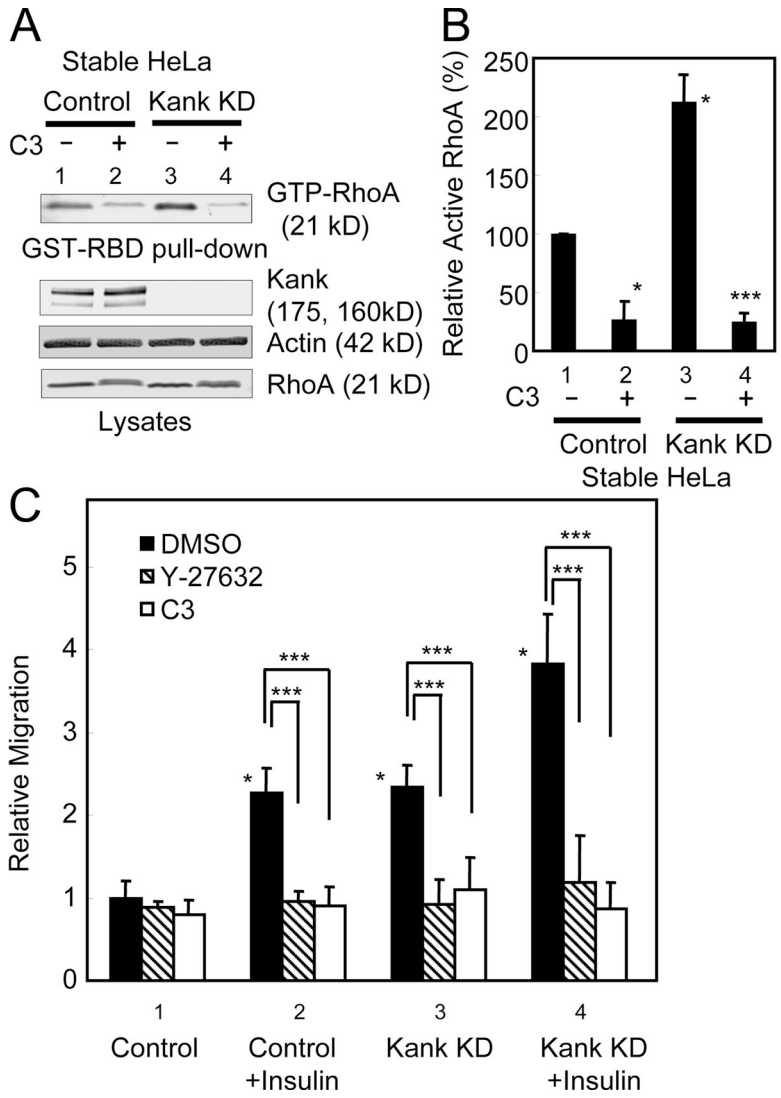

Figure 7. **Knockdown of Kank enhances RhoA-dependent cell migration.** (A and B) HeLa cells with stable knockdown of Kank (Kank KD) show increased activation of RhoA, whereas this activation is significantly blocked by cell-permeable C3 transferase. Stable Kank KD or control cells were treated with 1 µg/ml of cell-permeable C3 transferase and analyzed by GST-RBD pull-down assays. The levels of active RhoA were quantified and the relative levels compared with the control (lane 1) are shown in B. The results shown are the means ± SD of triplicate experiments. *, $P < 0.01$ compared with the control; ***, $P < 0.01$ compared with the control and the stable Kank KD. (C) Cell migration induced by 10 µg/ml insulin or Kank KD is inhibited by 2.5 µg/ml of cell-permeable C3 transferase and 10 µM Y-27632. The cells were treated as indicated and the cell migration assay was performed as described in Fig. 5. The results shown are the means ± SD of triplicate experiments. *, $P < 0.01$ compared with the control; ***, $P < 0.01$ compared as indicated.

bind to 14-3-3, and this interaction inhibits cofilin activity and enhances actin polymerization (Gohla and Bokoch, 2002; Birkenfeld et al., 2003; Soosairajah et al., 2005). Therefore, 14-3-3 may be important for the regulation of actin polymerization and the function of RhoA. We found that Kank inhibited RhoA activation and that this effect is caused by the interaction between Kank and 14-3-3, which is controlled by PI3K–Akt signaling (Figs. 6 and 7). When the cells are stimulated by growth factors, PI3K–Akt signaling also activates RhoA (Qian et al., 2004). Simultaneously, the interaction between Kank and 14-3-3 may be enhanced by growth factors (Fig. 3) and may result in the inactivation of RhoA (Fig. 6, H and I). Moreover, cell migration may be regulated by the interaction between Kank and 14-3-3 through RhoA inhibition (Figs. 5, 6, 7, S2, and S3). Fig. 8 shows a hypothetical model of Kank function in RhoA regulation. Stimulation by growth factors such as insulin activates the PI3K–Akt signal. The 14-3-3 complex, downstream of Akt or, alternatively, of other signaling pathways, activates RhoA. When cells need to negatively regulate the migration or change the direction of their migration, Akt phosphorylates Kank at S167, and Kank sequesters 14-3-3 from the active 14-3-3 complex. As a result, the amount of active RhoA is decreased and the cells can negatively regulate their migration by decelerating the formation of actin stress fibers. This scheme would be effective when there are excess signals from Akt to RhoA. Furthermore, because $Kank^{\Delta coil}$, which lacked a coiled-coil domain containing an IRSp53-binding site and a 14-3-3–binding motif, had no effect on actin stress fibers (Fig. 4), Kank function on actin stress fiber disorganization was not only dependent on 14-3-3 binding but also dependent on other proteins, and it is likely that there are additional mechanisms on actin stress fiber disorganization. Because the interaction between Kank and 14-3-3 did not affect the interaction between Kank and IRSp53 (Fig. S4, available at http://www.jcb.org/cgi/content/full/jcb.200707022/DC1), Kank function through 14-3-3 is different from Kank-IRSp53 function. At least, the Kank coiled-coil domain may be important to actin stress fiber regulation.

In conclusion, Kank is a novel Akt substrate and its interaction with 14-3-3 is controlled by the PI3K–Akt signal. This interaction regulates the activation of RhoA and inhibits the formation of actin stress fibers and cell migration. Kank is likely to be a protein negatively mediating the signal from

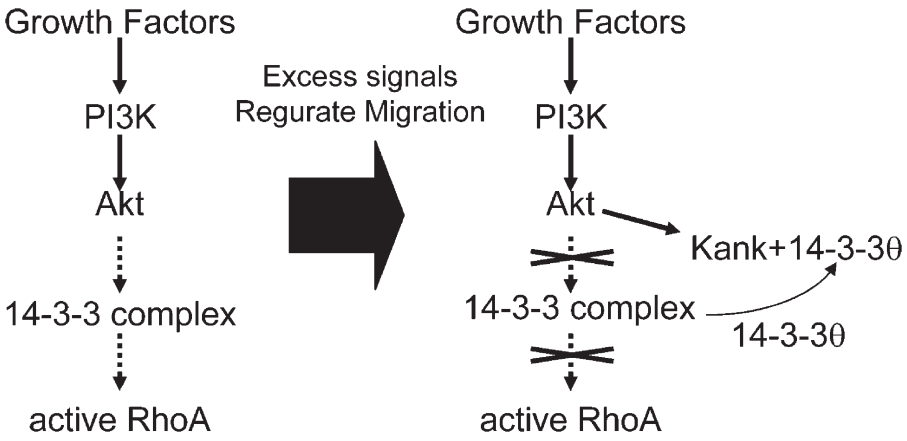

Figure 8. **A hypothetical model of RhoA regulation by Kank.** Growth factors such as insulin stimulate the PI3K–Akt signal. The 14-3-3 complex then activates RhoA, which is located downstream of the PI3K–Akt signal or other signaling pathways. When cells need to negatively regulate the migration, Kank is phosphorylated by Akt and sequesters 14-3-3θ from the 14-3-3 complex, resulting in suppression of active RhoA. Hypothetical pathways are indicated by hatched arrows.

PI3K–Akt to RhoA. However, the mechanism of activating RhoA by the PI3K–Akt signal has not been well investigated, and we do not know which RhoGEF or RhoGAP is functionally associated with Kank. Akt and p70S6K phosphorylate p122RhoGAP S322 (Hers et al., 2006). Hers et al. (2006) speculated that this phosphorylation inhibits RhoGAP activity and that the amount of active RhoA is increased. This Akt phosphorylation motif includes a candidate 14-3-3–binding motif. Therefore, there is a possibility that p122RhoGAP is one of the targets of Kank in the downstream of Akt. In fact, Kank binds to DLC1, a tumor suppressor and a human homologue of p122RhoGAP (unpublished data). However, Kank^{S167A} also binds to DLC1 (unpublished data), and the relationship between Kank and DLC1 through 14-3-3 has not been examined yet. Meanwhile, the expression of Kank is reduced or abrogated in RCC tissues and cell lines (Sarkar et al., 2002). As knockdown of Kank resulted in enhanced cell migration (Figs. 5 D, 7 C, and S3), this effect may be related to cancer progression. In addition, the deletion of the *Kank* region at 9p24 seems to be associated with familial cerebral palsy (Lerer et al., 2005). Therefore, Kank might be one of the targets for drug discovery for treatment of these diseases.

Materials and methods

Mammalian expression plasmids and stable cells

To generate FLAG-tagged Kank expression plasmids, the PCR products of Kank cDNA (GenBank/EMBL/DDBJ under accession No. NM_153186) were cloned into the EcoRI and SalI sites of pCMV-Tag2B (Stratagene), in which the FLAG tag was fused to the N terminus, or pCMV-Tag4A (Stratagene), in which the FLAG tag was fused to the C terminus. Point mutants and deletion mutants of Kank were generated by PCR. An expression plasmid of GFP-tagged human Kank or its mutants was generated by inserting the PCR products into pEGFP-C2 (Clontech Laboratories, Inc.). HA-tagged pcDNA3.1 was generated by inserting a short HA tag sequence into the NheI–EcoRI sites of the pcDNA3.1 vector (Invitrogen). 14-3-3 isoforms were cloned by RT-PCR using human kidney mRNA. HA-and GFP-tagged 14-3-3s were generated by subcloning each isoform into an HA-tagged pcDNA3.1 vector and a pEGFP-C2 vector, respectively. Active Akt was provided by T. Nakano and T. Kimura (Osaka University, Suita, Osaka, Japan; Watanabe et al., 2006). All plasmids were verified by sequencing.

The tetracycline-inducible stable HEK293 cells were generated by transfecting a pcDNA4/TO vector containing FLAG-Kank or FLAG-Kank^{S176A} into TREx-293 cells (Invitrogen). Tetracycline-inducible stable NIH3T3 cells were generated by transfecting a pcDNA6/TR vector (Invitrogen) and a pcDNA4/TO vector containing GFP-Kank or GFP-Kank^{S167A} into NIH3T3 cells. Tetracycline-inducible Kank-RNAi cells were generated by transfecting a pcDNA6/TR vector and a pSUPERIOR.zeosin vector containing a mouse sequence for knockdown of Kank as described below into NIH3T3 cells using an electroporation method. The pSUPERIOR.zeocin vector was generated from pSUPERIOR.neo+gfp (Oligoengine) by replacing the *neo-GFP* fusion gene with a *zeocin*-resistance gene. All tetracycline-inducible cell lines were cultured in media containing 150 µg/ml zeocin (Invitrogen) and 10 µg/ml blasticidin HCl (Invitrogen) and subjected to selection for 1 wk. The expression levels of Kank in the colonies after selection were checked by Western blotting. The stable Kank knockdown HeLa cell lines were generated by transfecting 15 µg of linearized pSUPER.neo vector containing a human sequence for knockdown of Kank as described below into HeLa cells using Gene Pulser II (Bio-Rad Laboratories) under conditions of 260 mV and 960 µF capacitance. After transfection, the cells were cultured in medium containing 500 µg/ml geneticin (Invitrogen) for 2 wk and clones were selected. Endogenous expression levels of Kank were checked by Western blotting.

Cell cultures

HEK293T, NIH3T3, and HeLa cells were cultured in DME. Renal carcinoma VMRC-RCW cells were cultured in MEM. HEK293 cells (provided by M. Noguchi, Hokkaido University, Sapporo, Hokkaido, Japan) were cultured in DME (high glucose). Mouse inner medullary collecting duct (IMCD) cells were cultured in DME/F-12 (1:1). All media used here, except when the cells were subjected to serum starvation, were supplemented with 10% FBS and streptomycin-kanamycin (Invitrogen). All cells were cultured at 37°C under a humidified atmosphere of 95% air and 5% CO_2.

Antibodies and reagents

Control rabbit IgG and control mouse IgG were obtained from Invitrogen and Santa Cruz Biotechnology, Inc., respectively. Anti-FLAG M2 mAb, anti–β-actin mAb, AP-conjugated goat anti–rabbit IgG, and insulin were obtained from Sigma-Aldrich. Anti-HA 12CA5 mAb, anti-MBP antisera, and anti-His mAb were obtained from Roche, New England Biolabs, Inc., and QIAGEN, respectively. Anti-AFP 3E6 mAb (Qbiogene) was used for immunoprecipitation of GFP fusion proteins and anti-GFP antiserum (Invitrogen) was used for Western blotting and immunofluorescence of GFP fusion proteins. The anti–human Kank mAb and polyclonal antibody (pAb) were described previously (Roy et al., 2005; Sarkar et al., 2002). The anti–mouse Kank pAb recognized amino acids 861–975. 14-3-3θ mAb and 14-3-3pan pAb were obtained from Exalpha Biologicals, Inc., and Delta Biolabs LLC, respectively. Anti-GST 26H1 mAb, anti–phosho-Akt pAb, anti-Akt pAb, anti–phospho-p70S6K pAb, anti-p70S6K pAb, HRP-linked goat anti–rabbit IgG, HRP-linked goat anti–mouse IgG, and AP-conjugated goat anti–mouse IgG were obtained from Cell Signaling Technology. Alexa Fluor 488 goat anti–rabbit IgG, Alexa Fluor 488 goat anti–mouse IgG, and Alexa Fluor 596 goat anti–rabbit IgG were obtained from Invitrogen. Cy5-conjugated goat anti–mouse IgG was obtained from Millipore. Calyculin A and wortmannin were purchased from BIOMOL International, L.P. EGF and ECL cell attachment matrix were obtained from Millipore. LY294002, rapamycin, and Y-27632 were obtained from EMD. HRP-conjugated streptavidin was obtained from Invitrogen.

Knockdown of Kank

An H1 promoter-based mammalian expression vector, pSUPER.neo (Oligoengine), was used for transient and stable expression of siRNA in NIH3T3

cells and human cell lines. A 19-nucleotide sequence corresponding to nucleotides 609–627 (5′-GAGGCGAAAGCCATCTGTG-3′) of a mouse cDNA clone, A530060J16 (GenBank/EMBL/DDBJ under accession No. AK041011.1), was used for RNAi for mouse *Kank*, and a 19-nucleotide sequence corresponding to nucleotides 2,043–2,262 (5′-GTGACCGTCT-GCTCTCCAA-3′) of human *Kank* cDNA (GenBank/EMBL/DDBJ under accession No. NM_015158) was used for RNAi for human *Kank*. *Kank*-esiRNA was prepared as described previously (Kittler et al., 2004; Yang et al., 2002). In brief, sense and antisense RNA was transcribed from human *Kank* plasmids using a T7 promoter system (for both strands) supplied in a MEGAscript kit (Ambion). After annealing the sense and antisense strands, RNA was treated with ShortCut RNase III (New England Biolabs, Inc.) and purified with Sepharose Q (GE Healthcare). *Kank* esiRNA and control esiRNA containing the *Xenopus laevis* elongation factor gene was transfected into HEK293 cells using Lipofectamine 2000 (Invitrogen) according to the manufacturer's instructions.

In vitro binding assay

The coiled-coil domain of Kank and its mutant containing S167A were generated by using a TNT-coupled reticulocyte lysate system with biotinylated Lys-tRNA (Promega) and mixed with bacterially expressed GST-tagged 14-3-3 isoforms. These protein complexes were pulled down with glutathione–Sepharose 4B and subjected to SDS-PAGE followed by Western blotting. The bands were detected using HRP-conjugated streptavidin.

In vitro phosphorylation assays

In vitro phosphorylation assays were performed using Akt/PKB protein kinase (Cell Signaling Technology) with [γ-^{32}P]ATP according to the manufacturer's instructions. GST-GSK3β was used as a positive control for phosphorylation by Akt.

Immunocytochemistry

The cells grown on glass coverslips were washed three times with PBS and fixed with 3.7% formaldehyde/PBS for 30 min at room temperature or cold methanol for 15 min at –20°C. After the cells were treated with 0.25% Triton X-100 for 10 min at room temperature, they were incubated with the appropriate antibodies. After washing with PBS, the cells were incubated with the indicated secondary antibodies. F-actin was stained using TRITC-conjugated phalloidin (Sigma-Aldrich). Fluorochromes used are indicated in figure legends. Images of cells mounted at room temperature in 80% (wt/vol) glycerol in PBS were acquired with AxioVision 3.1 (Carl Zeiss, Inc.) using a fluorescence microscope (Axioskop 2 plus; Carl Zeiss, Inc.) with a Plan-Neofluar 40× NA 0.75 objective (Carl Zeiss, Inc.) and a color camera (AxioCam HRc; Carl Zeiss, Inc.). Images were prepared with Photoshop 7.0 (Adobe).

Cell migration assay

Cell migration assays were performed as described previously with some modifications (Praus et al., 1999). In brief, transfection was performed using Lipofectamine 2000 (Invitrogen) 1 d before the assay. Tetracycline induction was started 24 h before the assay. TransWells (Corning Incorporated) were precoated with ECL cell attachment matrix before use and cells (5×10^4) were seeded in the upper chamber and incubated for 16 h. The cells were then fixed and stained with Mayer's Hematoxylin (Wako Pure Chemical Industries, Ltd.). Migrated cells in 10 randomly chosen fields of each well were counted. Each experiment was performed at least three times.

GST-RBD pull-down assays

GST-RBD pull-down assays were performed as described previously (Diviani et al., 2004). In brief, the cells were lysed in ice-cold lysis buffer containing 0.1% SDS. The cell lysates were centrifuged and the concentrations of protein in the supernatants were quantified with a DC protein assay kit (Bio-Rad Laboratories). Equal amounts of proteins were pulled down with GST-RBD and glutathione–Sepharose 4B for 1 h at 4°C. The precipitates were washed five times with the 0.1% SDS lysis buffer and subjected to Western blotting. The bands were quantified using ImageQuant software (Molecular Dynamics).

Online supplemental material

Fig. S1 shows that Kank negatively regulates F-actin. Fig. S2 shows that Kank inhibits cell migration through 14-3-3 in HEK293 cells. Fig. S3 shows that Kank inhibits RhoA-dependent cell migration in HEK293 cells. Fig. S4 shows that the interaction between Kank and IRSp53 is only slightly affected by 14-3-3. Online supplemental material is available at http://www.jcb.org/cgi/content/full/jcb.200707022/DC1.

We thank Prof. M. Noguchi (Hokkaido University), for providing HEK293 cells and Prof. T. Nakano and Dr. T. Kimura (Osaka University) for providing an active Akt construct. We also thank Prof. T. Akiyama and Dr. Y. Kawasaki for providing materials and helpful advice.

This work was supported by the Special Coordination Fund for Promoting Science and Technology by the Ministry of Education, Culture, Sports, Science and Technology of Japan and by a fund for promoting collaboration with small and medium enterprises from the National Institute of Advanced Industrial Science and Technology.

Submitted: 5 July 2007
Accepted: 4 April 2008

References

Alessi, D.R., M. Andjelkovic, B. Caudwell, P. Cron, N. Morrice, P. Cohen, and B.A. Hemmings. 1996. Mechanism of activation of protein kinase B by insulin and IGF-1. *EMBO J.* 15:6541–6551.

Amano, M., Y. Fukata, and K. Kaibuchi. 2000. Regulation and functions of Rho-associated kinase. *Exp. Cell Res.* 261:44–51.

Aoki, M., C. Schetter, M. Himly, O. Batista, H.W. Chang, and P.K. Vogt. 2000. The catalytic subunit of phosphoinositide 3-kinase: requirements for oncogenicity. *J. Biol. Chem.* 275:6267–6275.

Bellacosa, A., J.R. Testa, S.P. Staal, and P.N. Tsichlis. 1991. A retroviral oncogene, akt, encoding a serine-threonine kinase containing an SH2-like region. *Science.* 254:274–277.

Birkenfeld, J., H. Betz, and D. Roth. 2003. Identification of cofilin and LIM-domain containing protein kinase 1 as novel interaction partners of 14-3-3ζ. *Biochem. J.* 369:45–54.

Bonnefoy-Bérard, N., Y.C. Liu, M. von Willebrand, A. Sung, C. Elly, T. Mustelin, H. Yoshida, K. Ishizaka, and A. Altman. 1995. Inhibition of phosphatidylinositol 3-kinase activity by association with 14-3-3 proteins in T cells. *Proc. Natl. Acad. Sci. USA.* 92:10142–10146.

Chang, H.W., M. Aoki, D. Fruman, K.R. Auger, A. Bellacosa, P.N. Tsichlis, L.C. Cantley, T.M. Roberts, and P.K. Vogt. 1997. Transformation of chicken cells by the gene encoding the catalytic subunit of PI 3-kinase. *Science.* 276:1848–1850.

Craparo, A., R. Freund, and T.A. Gustafson. 1997. 14-3-3(ε) interacts with the insulin-like growth factor I receptor and insulin receptor substrate I in an phosphoserine-dependent manner. *J. Biol. Chem.* 272:11663–11669.

Cross, D.A.E., D.R. Alessi, P. Cohen, M. Andjelkovich, and B.A. Hemmings. 1995. Inhibition of glycogen synthase kinase-3 by insulin mediated by protein kinase B. *Nature.* 378:785–789.

Datta, S.R., H. Dudek, X. Tao, S. Masters, H. Fu, Y. Gotoh, and M.E. Greenberg. 1997. Akt phosphorylation of BAD couples survival signals to the cell-intrinsic death machinery. *Cell.* 91:231–241.

Ding, M., A. Goncharov, Y. Jin, and A.D. Chisholm. 2003. *C. elegans* ankyrin repeat protein VAB-19 is a component of epidermal attachment structures and is essential for epidermal morphogenesis. *Development.* 130:5791–5801.

Diviani, D., L. Abuin, S. Cotecchia, and L. Pansier. 2004. Anchoring of both PKA and 14-3-3 inhibits the Rho-GEF activity of the AKAP-Lbc signaling complex. *EMBO J.* 23:2811–2820.

Dudek, H., S.R. Datta, T.F. Franke, M.J. Birnbaum, R. Yao, G.M. Cooper, R.A. Segal, D.R. Kaplan, and M.E. Greenberg. 1997. Regulation of neuronal survival by the serine-threonine protein kinase Akt. *Science.* 275:661–665.

Enomoto, A., H. Murakami, N. Asai, N. Morone, T. Watanabe, K. Kawai, Y. Murakumo, J. Usukura, K. Kaibuchi, and M. Takahashi. 2005. Akt/PKB regulates actin organization and cell motility via Girdin/APE. *Dev. Cell.* 9:389–402.

Franke, T.F., S.-I. Yang, T.O. Chan, K. Datta, A. Kazlauskas, D.K. Morrison, D.R. Kaplan, and P.N. Tsichlis. 1995. The protein kinase encoded by the *Akt* proto-oncogene is a target of the PDGF-activated phosphatidylinositol 3-kinase. *Cell.* 81:727–736.

Fukata, Y., M. Amano, and K. Kaibuchi. 2001. Rho-Rho-kinase pathway in smooth muscle contraction and cytoskeletal reorganization of non-muscle cells. *Trends Pharmacol. Sci.* 22:32–39.

Fulton, D., J.P. Gratton, T.J. McCabe, J. Fontana, Y. Fujio, K. Walsh, T.F. Franke, A. Papapetropoulos, and W.C. Sessa. 1999. Regulation of endothelium-derived nitric oxide production by the protein kinase Akt. *Nature.* 399:597–601.

Furnari, F.B., H.J. Huang, and W.K. Cavenee. 1998. The phosphoinositol phosphatase activity of *PTEN* mediates a serum-sensitive G_1 growth arrest in glioma cells. *Cancer Res.* 58:5002–5008.

Gohla, A., and G.M. Bokoch. 2002. 14-3-3 regulates actin dynamics by stabilizing phosphorylated cofilin. *Curr. Biol.* 12:1704–1710.

Han, D.C., L.G. Rodriguez, and J.L. Guan. 2001. Identification of a novel interaction between integrinß1 and 14-3-3β. *Oncogene.* 20:346–357.

Hers, I., M. Wherlock, Y. Homma, H. Yagisawa, and J.M. Tavaré. 2006. Identification of p122RhoGAP (deleted in liver cancer-1) Serine 322 as a substrate for protein kinase B and ribosomal S6 kinase in insulin-stimulated cells. *J. Biol. Chem.* 281:4762–4770.

Hsu, S.Y., A. Kaipia, L. Zhu, and A.J.W. Hsueh. 1997. Interference of BAD (Bcl-xL/Bcl-2-associated death promoter)-induced apoptosis in mammalian cells by 14-3-3 isoforms and P11. *Mol. Endocrinol.* 11:1858–1867.

Itoh, K., K. Yoshioka, H. Akedo, M. Uehata, T. Ishizaki, and S. Narumiya. 1999. An essential part for Rho-associated kinase in the transcellular invasion of tumor cells. *Nat. Med.* 5:221–225.

Jin, J., F.D. Smith, C. Stark, C.D. Wells, J.P. Fawcett, S. Kulkarni, P. Metalnikov, P. O'Donnell, P. Taylor, L. Taylor, et al. 2004. Proteomic, functional, and domain-based analysis of in vivo 14-3-3 binding proteins involved in cytoskeletal regulation and cellular organization. *Curr. Biol.* 14:1436–1450.

Karnam, P., M.L. Standaert, L. Galloway, and R.V. Farese. 1997. Activation and translocation of Rho (and ADP ribosylation factor) by insulin in rat adipocytes. *J. Biol. Chem.* 272:6136–6140.

Kittler, R., G. Putz, L. Pelletier, I. Poser, A.K. Heninger, D. Drechsel, S. Fischer, I. Konstantinova, B. Habermann, H. Grabner, et al. 2004. An endoribonuclease-prepared siRNA screen in human cells identifies genes essential for cell division. *Nature.* 432:1036–1040.

Kurokawa, K., and M. Matsuda. 2005. Localized RhoA activation as a requirement for the induction of membrane ruffling. *Mol. Biol. Cell.* 16:4294–4303.

Lerer, I., M. Sagi, V. Meiner, T. Cohen, J. Zlotogora, and D. Abeliovich. 2005. Deletion of the *ANKRD15* gene at 9p24.3 causes parent-of-origin-dependent inheritance of familial cerebral palsy. *Hum. Mol. Genet.* 14:3911–3920.

Li, S., P. Janosch, M. Tanji, G.C. Rosenfeld, J.C. Waymire, H. Mischak, W. Kolch, and J.M. Sedivy. 1995. Regulation of Raf-1 kinase activity by the 14-3-3 family proteins. *EMBO J.* 14:685–696.

Lottersberger, F., A. Panza, G. Lucchini, S. Piatti, and M.P. Longhese. 2006. The *Saccharomyces cerevisiae* 14-3-3 proteins are required for the G1/S transition, actin cytoskeleton organization and cell wall integrity. *Genetics.* 173:661–675.

Maekawa, M., T. Ishizaki, S. Boku, N. Watanabe, A. Fujita, A. Iwamatsu, T. Obinata, K. Ohashi, K. Mizuno, and S. Narumiya. 1999. Signaling from Rho to the actin cytoskeleton through protein kinases ROCK and LIM-kinase. *Science.* 285:895–898.

Mhawech, P. 2005. 14-3-3 proteins—an update. *Cell Res.* 15:228–236.

Muslin, A.J., J.W. Tanner, P.M. Allen, and A.S. Shaw. 1996. Interaction of 14-3-3 with signaling proteins is mediated by the recognition of phosphoserine. *Cell.* 84:889–897.

Nobes, C.D., and A. Hall. 1995. Rho, Rac, and Cdc42 GTPases regulate the assembly of multimolecular focal complexes associated with actin stress fibers, lamellipodia, and filopodia. *Cell.* 81:53–62.

Okano, J., I. Gaslightwala, M.J. Birnbaum, A.K. Rustgi, and H. Nakagawa. 2000. Akt/protein kinase B isoforms are differentially regulated by epidermal growth factor stimulation. *J. Biol. Chem.* 275:30934–30942.

Oksvold, M.P., H.S. Huitfeldt, and W.Y. Langdon. 2004. Identification of 14-3-3ζ as an EGF receptor interacting protein. *FEBS Lett.* 569:207–210.

Paterson, H.F., A.J. Self, M.D. Garrett, I. Just, K. Aktories, and A. Hall. 1990. Microinjection of recombinant p21rho induces rapid changes in cell morphology. *J. Cell Biol.* 111:1001–1007.

Pozuelo Rubio, M., K.M. Geraghty, B.H.C. Wong, N.T. Wood, D.G. Campbell, N. Morrice, and C. Mackintosh. 2004. 14-3-3-affinity purification of over 200 human phosphoproteins reveals new links to regulation of cellular metabolism, proliferation and trafficking. *Biochem. J.* 379:395–408.

Praus, M., K. Wauterickx, D. Collen, and R.D. Gerard. 1999. Reduction of tumor cell migration and metastasis by adenoviral gene transfer of plasminogen activator inhibitors. *Gene Ther.* 6:227–236.

Qian, Y., L. Corum, Q. Meng, J. Blenis, J.Z. Zheng, X. Shi, D.C. Flynn, and B.H. Jiang. 2004. PI3K induced actin filament remodeling through Akt and p70S6K1: implication of essential role in cell migration. *Am. J. Physiol. Cell Physiol.* 286:C153–C163.

Qiang, Y.W., L. Yao, G. Tosato, and S. Rudikoff. 2004. Insulin-like growth factor I induces migration and invasion of human multiple myeloma cells. *Blood.* 103:301–308.

Ridley, A.J., and A. Hall. 1992. The small GTP-binding protein rho regulates the assembly of focal adhesions and actin stress fibers in response to growth factors. *Cell.* 70:389–399.

Ridley, A.J., M.A. Schwartz, K. Burridge, R.A. Firtel, M.H. Ginsberg, G. Borisy, J.T. Parsons, and A.R. Horwitz. 2003. Cell migration: integrating signals from front to back. *Science.* 302:1704–1709.

Rodriguez, L.G., and J.L. Guan. 2005. 14-3-3 regulation of cell spreading and migration requires a functional amphipathic groove. *J. Cell. Physiol.* 202:285–294.

Roth, D., J. Birkenfeld, and H. Betz. 1999. Dominant-negative alleles of 14-3-3 proteins cause defects in actin organization and vesicle targeting in the yeast *Saccharomyces cerevisiae. FEBS Lett.* 460:411–416.

Roy, B.C., T. Aoyagi, S. Sarkar, K. Nomura, H. Kanda, K. Iwaya, M. Tachibana, and R. Kiyama. 2005. Pathological characterization of *Kank* in renal cell carcinoma. *Exp. Mol. Pathol.* 78:41–48.

Sarkar, S., B.C. Roy, N. Hatano, T. Aoyagi, K. Gohji, and R. Kiyama. 2002. A novel ankyrin repeat-containing gene *(Kank)* located at 9p24 is a growth suppressor of renal cell carcinoma. *J. Biol. Chem.* 277:36585–36591.

Scita, G., P. Tenca, E. Frittoli, A. Tocchetti, M. Innocenti, G. Giardina, and P.P. Di Fiore. 2000. Signaling from Ras to Rac and beyond: not just a matter of GEFs. *EMBO J.* 19:2393–2398.

Sekimoto, T., M. Fukumoto, and Y. Yoneda. 2004. 14-3-3 suppresses the nuclear localization of threonine 157-phosphorylated $p27^{kip1}$. *EMBO J.* 23:1934–1942.

Shanley, L.J., C.D. McCaig, J.V. Forrester, and M. Zhao. 2004. Insulin, not leptin, promotes in vitro cell migration to heal monolayer wounds in human corneal epithelium. *Invest. Ophthalmol. Vis. Sci.* 45:1088–1094.

Shin, I., F.M. Yakes, F. Rojo, N.Y. Shin, A.V. Bakin, J. Baselga, and C.L. Arteaga. 2002. PKB/Akt mediates cell-cycle progression by phosphorylation of p27 (Kip1) at threonine 157 and modulation of its cellular localization. *Nat. Med.* 8:1145–1152.

Soosairajah, J., S. Maiti, O. Wiggan, P. Sarmiere, N. Moussi, B. Sarcevic, R. Sampath, J.R. Bamburg, and O. Bernard. 2005. Interplay between components of a novel LIM kinase-slingshot phosphatase complex regulates cofilin. *EMBO J.* 24:473–486.

Staal, S.P. 1987. Molecular cloning of the *akt* oncogene and its human homologues *AKT1* and *AKT2*: Amplification of *AKT1* in a primary human gastric adenocarcinoma. *Proc. Natl. Acad. Sci. USA.* 84:5034–5037.

Takaishi, K., A. Kikuchi, S. Kuroda, K. Kotani, T. Sasaki, and Y. Takai. 1993. Involvement of *rho* p21 and its inhibitory GDP/GTP exchange protein (*rho* GDI) in cell motility. *Mol. Cell. Biol.* 13:72–79.

Wallar, B.J., and A.S. Alberts. 2003. The formins: active scaffolds that remodel the cytoskeleton. *Trends Cell Biol.* 13:435–446.

Watanabe, S., H. Umehara, K. Murayama, M. Okabe, T. Kimura, and T. Nakano. 2006. Activation of Akt signaling is sufficient to maintain pluripotency in mouse and primate embryonic stem cells. *Oncogene.* 25:2697–2707.

Worthylake, R.A., and K. Burridge. 2003. RhoA and ROCK promote migration by limiting membrane protrusions. *J. Biol. Chem.* 278:13578–13584.

Yaffe, M.B., G.G. Leparc, J. Lai, T. Obata, S. Volinia, and L.C. Cantley. 2001. A motif-based profile scanning approach for genome-wide prediction of signaling pathways. *Nat. Biotechnol.* 19:348–353.

Yang, D., F. Buchholz, Z. Huang, A. Goga, C.Y. Chen, F.M. Brodsky, and J.M. Bishop. 2002. Short RNA duplexes produced by hydrolysis with *Escherichia coli* RNase III mediate effective RNA interference in mammalian cells. *Proc. Natl. Acad. Sci. USA.* 99:9942–9947.

Yoshioka, K., S. Nakamori, and K. Itoh. 1999. Overexpression of small GTP-binding protein RhoA promotes invasion of tumor cells. *Cancer Res.* 59:2004–2010.

Zhai, J., H. Lin, M. Shamim, W.W. Schlaepfer, and R. Cañete-Soler. 2001. Identification of a novel interaction of 14-3-3 with p190RhoGEF. *J. Biol. Chem.* 276:41318–41324.